Mapping of Interception Loss of Vegetation in the Heihe River Basin of China Using Remote Sensing Observations

Yaokui Cui, Li Jia, Guangcheng Hu, and Jie Zhou

***Abstract*—Interception loss is an important component of the regional water balance for the Heihe River Basin which is an inland basin with limited precipitation. We used a modified Gash analytical model by combining remote sensing observations to estimate the interception loss of several vegetation types, e.g., grass, crop, forest and shrub for the years 2003–2012 in the Heihe River Basin. The estimated monthly interception ratio (in percent) was compared with field measurements made in Dayekou and Pailugou forest hydrology experimental sites and the results showed reasonable accuracy with RMSE of 5.0% and 4.3% at the two sites, respectively. The regional distribution of the interception loss showed strong spatial and temporal variability at monthly scale. At annual scale, the interception ratio could be treated as a stable indicator for long-term water balance research. The annual average interception loss is about 7.2% of gross rainfall for the vegetation covered area in the Heihe River Basin.**

***Index Terms*—Heihe River Basin, interception loss, remote sensing, RS-Gash model.**

I. Introduction

EVAPOTRANSPIRATION (ET), including evaporation (E) and transpiration (T), is a vital component of the water cycle and plays an important role in planning and monitoring of consumptive water use [1]. Interception loss can be considered as a quantity, defined as the rainfall intercepted by a surface and subsequently evaporated back to the atmosphere [2]. Previous studies have found that the magnitude of interception loss of vegetation is in the range of 8–40% of annual gross rainfall according to field observations [3]–[5]. Consequently, models ignoring interception loss of vegetation may underestimate ET from vegetated land [6], [7].

Manuscript received January 31, 2014; revised April 18, 2014; accepted May 10, 2014. This work was supported in part by the National Science Foundation of China under Grants 91025004 and 41101331 and the National High Technology Research and Development Program of China under Grant 2012AA12A304. *(Corresponding author: L. Jia.)*

Y. Cui and J. Zhou are with the State Key Laboratory of Remote Sensing Science, Institute of Remote Sensing and Digital Earth, Chinese Academy of Sciences, Beijing 100101, China and also with the University of Chinese Academy of Sciences, Beijing 100049, China.

L. Jia is with the State Key Laboratory of Remote Sensing Science, Institute of Remote Sensing and Digital Earth, Chinese Academy of Sciences, Beijing 100101, China and also with Joint Center for Global Change Studies, Beijing 100875, China (e-mail: jiali@radi.ac.cn).

G. Hu is with the State Key Laboratory of Remote Sensing Science, Institute of Remote Sensing and Digital Earth, Chinese Academy of Sciences, Beijing 100101, China.

Color versions of one or more of the figures in this paper are available online at http://ieeexplore.ieee.org.

Digital Object Identifier 10.1109/LGRS.2014.2324635

Until now, many studies on the interception loss have focused on field scale [3], [5], [8], [9]. These methods or achievements cannot be used directly at basin scales, since land surface is often characterized as heterogeneous and the spatial distribution of vegetation is complex at this scale. To improve the observability of hydrological and ecological processes, and to enhance the applicability of remote sensing in integrated eco-hydrological studies and water resources management at basin scale, Watershed Allied Telemetry Experimental Research (WATER) [10] and Heihe Watershed Allied Telemetry Experimental Research (HiWATER) [11] were carried out in the Heihe River Basin. In this letter, we pay more attention to the interception loss at monthly and annual temporal scales in the Heihe River Basin. A recently developed modified Gash model [12] was applied using remotely sensed vegetation canopy parameters and precipitation to estimate the interception loss of the main vegetation types in the Heihe River Basin. Time series maps of interception loss between 2003 and 2012 in this region are created. Spatial and temporal variability of interception loss of the main vegetation types at monthly and annual temporal scales are further analyzed. Finally, some issues about the estimation of regional interception loss using remote sensing observations are discussed.

II. Study Area and Data

A. Study Area

The study area is the Heihe River Basin which is located in latitude 37.73°–42.69° N and longitude 97.13°–101.98° E in an arid region of northwest China (Fig. 1). The elevations vary from about 5000 m in the Heihe upper reaches to 1500 m in the middle reaches. The landscapes are diverse and the main vegetation types are grass (54%), crop (22.5%), forest (14.3%), and shrub (7%). The distribution of precipitation in this region shows a strong spatial heterogeneity and varies from 400–600 mm/yr in the Heihe upper reaches to less than 200 mm/yr in the middle reaches and even much less (smaller than 50 mm/yr) in the lower reaches [11].

B. Data

The meteorological data, including hourly near surface air temperature (T_{air}), air pressure (P), and relative humidity (RH) at 2 m height, wind speed at 10 m height (U), downward shortwave radiation flux $(R_s^{\downarrow})$, and downward longwave radiation flux $(R_l^{\downarrow})$ were obtained using Weather Research and Forecasting (WRF) model [13].

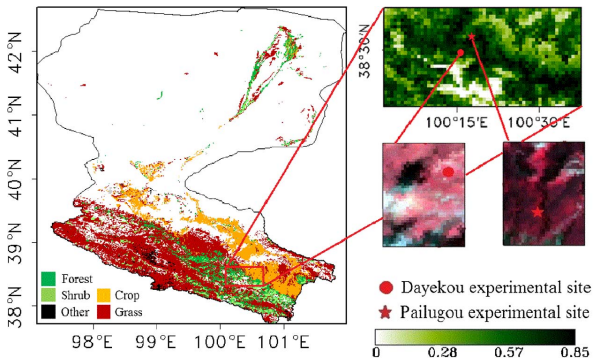

Fig. 1. Vegetation classification map of the Heihe River Basin (big map on the left) and maps of Dayekou and Pailugou experimental sites (big map on the upper-right created using MODIS NDVI on June 27, 2008 and the two small false color images on the middle-right created using the Hyperion image on June 15, 2008 with a resolution of 30 m). The two false color images on the right represent one MODIS pixel ($0.01^\circ \times 0.01^\circ$) surrounding the two sites respectively.

The gap-free Normalized Difference Vegetation Index (NDVI) and Leaf Area Index (LAI) data set with 0.01° in spatial and 8-day in temporal resolution are reconstructed from Moderate Resolution Imaging Spectroradiometer (MODIS) products of NDVI (MOD13A2) and LAI (MOD15A2), respectively using an algorithm developed in [14]. The land cover product used in this study is based on the International Geosphere Biosphere Programme (IGBP) classification scheme [15]. The data sets are provided by the "Heihe Plan Science Data Center" and can be downloaded at http://www.heihedata.org.

The products of the Tropical Rainfall Measuring Mission (TRMM) 3B42 Version 7 (V7), with a temporal resolution of 3-hour and a spatial resolution of 0.25° were used as precipitation data. For TRMM 3B42 products, which merged TRMM and other sources precipitation estimates, do not distinguish between rain and snow [19] and the precipitation is small in the winter for our study area, we treat them as rainfall data when calculating the interception loss and the error due to this might have limited influence on annual interception loss. The daily precipitation was obtained by summing up all eight sets of 3-hourly TRMM precipitation. Linear interpolation method was used to obtain data at a finer spatial resolution of 0.01°.

The interception loss was measured at two forest experimental sites in Heihe River Basin (Fig. 1) from June to September in 2008. One site is Dayekou forest hydrology experimental site (100.258° E, 38.507° N) with one experimental plot, and the other is Pailugou forest hydrology experimental site (100.295° E, 38.543° N) with three experimental plots [10]. The forests are dominated by *Picea crassifolia*. Interception ratio (percentage of the interception over gross rainfall) is used to evaluate the performance of our model.

An Earth Observing-1 (EO-1) Hyperion image with a resolution of 30 m on June 15, 2008 was used to calculate the fraction of forest in the MODIS pixel covering the experimental site for validation study.

III. Methods

A. RS-Gash Model for Interception Loss Estimation

The RS-Gash model (Remote Sensing based Gash model) [12], a recently developed modified Gash model for interception loss estimation using remote sensing observations at regional scale, is applied in this letter to estimate interception loss of various vegetation types in the Heihe River Basin. Only major equations of the RS-Gash model are given below, the readers are encouraged to read the full description of the model in Cui and Jia [12].

In the RS-Gash model, a pixel of remote sensing image is divided into several subpixels using Poisson distribution function to depict the subpixel heterogeneity of vegetation density, so as to interception loss. The RS-Gash model works under two assumptions that there is only one storm per rainy day so that it could be used on a daily scale and there is only a fraction of saturated vegetation, which corresponds to cases without very heavy rainfall [12].

At pixel scale, the interception loss, I (mm), is the integration of all subpixels by the Poisson distribution probability

$$I = \sum_{i=1}^{n} Pb_i \cdot I_i \tag{1}$$

where I_i (mm) is the interception loss of the ith subpixel, and Pb_i is the corresponding probability which is given by Poisson distribution function.

At subpixel scale, the threshold value of precipitation required to saturate the vegetation $P'_{G,i}$ (mm) is given by

$$P'_{G,i} = -\frac{\overline{R}}{\overline{E_V}} \cdot \frac{S_{veg}}{FVC} \cdot \ln\left(1 - \frac{\overline{E_V}}{\overline{R}}\right) \tag{2}$$

$$S_{veg} = S_V \cdot VAI \tag{3}$$

where $\overline{E_V}$ (mm h^{-1}) is the mean evaporation rate per unit vegetation coverage area from saturated vegetation surfaces, including evaporation rate from canopy and stem; $\overline{R}$ (mm h^{-1}) is the mean rainfall rate which is larger enough to make the vegetation saturated; the ratio of $\overline{E_V}$ over $\overline{R}$ is monthly mean and obtained for every month, and assumed to be equal for all storms during one month; FVC is the Fractional Vegetation Cover; VAI (m^2 m^{-2}) is the Vegetation Area Index (one-sided area) including all parts of vegetation, such as green leaves, dry leaves, branches, stem and trunk; S_{veg} (mm) is vegetation storage capacity, including canopy and stem storage capacity, which is assumed linearly related with VAI; S_V (mm) is the specific vegetation storage, defined as the depth of water retained by vegetation per unit vegetation area. The values of S_V for different IGBP vegetation types are given in Table I, which are statistical average of the same vegetation type taken from the literature [3] and can represent most vegetation types.

The interception loss of vegetation in subpixel is calculated as

$$\begin{cases} I_i = FVC \cdot P_G & \text{for } \left(P_G \le P'_{G,i}\right) \\ I_i = FVC \cdot P'_{G,i} \\ \quad + \left(FVC \cdot \overline{E_V}/\overline{R}\right)\left(P_G - P'_{G,i}\right) & \text{for } \left(P_G > P'_{G,i}\right) \end{cases} \tag{4}$$

where P_G (mm) is the gross rainfall.

The monthly interception loss is obtained by summing up all results of daily interception loss for a given month, and the same to annual interception loss.

TABLE I
PARAMETERS USED IN THIS WORK

IGBP Code	Vegetation Types	h (m)	$L_{s,\min}$ (m^2 m^{-2})	β	S_V
1,3	Needleleaf Forests	8	1×max(FVC)	0.85	0.25
4	Broadleaf Forests	8	1×max(FVC)	0.85	0.15
5	Mixed Forests	8	1×max(FVC)	0.85	0.2
6,7	Shrublands	2	1×max(FVC)	0.85	0.55
10	Grasslands	0.3×$NDVI$	0.5×max(FVC)	0.85	0.06
11	Permanent Wetlands	2×$NDVI$	0.1×max(FVC)	0.85	0.06
12	Croplands	2×$NDVI$	0.1×max(FVC)	0.9	0.06
14	Cropland/Natural Vegetation Mosaic	2×$NDVI$	0.5×max(FVC)	0.9	0.06

As a modified Gash model, the RS-Gash model extends the original Gash model from point scale to the regional scale by introducing two new items: using S_{veg} to introduce trunk storage capacity in the total vegetation storage capacity, and using FVC to introduce the trunk evaporation in the total evaporation. In addition, the heterogeneity of interception loss within pixel is also considered by applying the Poisson distribution function to satellite observed LAI at each pixel [12].

B. Mean Evaporation Rate of Saturated Vegetation

The mean evaporation rate $\overline{E_V}$ is calculated based on Penman–Monteith equation by setting the surface resistance to zero

$$\lambda E = (\Delta R_n + \rho c_p D/r_a)(\Delta + \gamma)^{-1} \tag{5}$$

where E (kg m^{-2} s^{-1}) is the evaporation rate; λ (J kg^{-1}) is the latent heat of vaporization; r_a (s m^{-1}) is the aerodynamic resistance; R_n (W m^{-2}) is the net radiation; c_p (J kg^{-1} K^{-1}) is the specific heat capacity of air at constant pressure; D (Pa) is the vapor pressure deficit; γ (Pa K^{-1}) is the psychrometric constant; Δ (Pa K^{-1}) is the slope of the saturation vapor pressure curve at air temperature; and ρ (kg m^{-3}) is the density of air.

The aerodynamic resistance r_a is calculated as

$$r_a = \ln\left((z-d)/z_0\right)^2/(\kappa^2 u) \tag{6}$$

where z (m) is the height of wind speed u (m s^{-1}) measurements; κ (0.41) is von Karman constant; the roughness length parameters are $d = 0.75 \cdot h$ and $z_0 = 0.1 \cdot h$, h (m) is the vegetation height which is given in Table I for different vegetation types. The h of forest and shrub are taken as constant values, and the h of grass and crop are assumed to be a linear function of NDVI.

The net radiation flux R_n is calculated by the equation

$$R_n = (1-\alpha)R_s^{\downarrow} + \varepsilon \cdot R_l^{\downarrow} - \delta \cdot \varepsilon \cdot T_s^4 \tag{7}$$

where α is the albedo of saturated vegetation and taken as a constant of 0.05; T_s (K) is the temperature of saturated vegetation and assumed to be equal to the air temperature during rainfall; δ (5.67×10^{-8} W m^{-2} K^{-4}) is Stefan–Boltzmann constant; ε is the emissivity of saturated vegetation and taken as 0.99.

C. VAI and FVC

The Vegetation Area Index VAI is calculated by [17]

$$VAI = LAI_g + L_s \tag{8}$$

where LAI_g (m^2 m^{-2}) is the green leaf area index and provided by MODIS LAI product; L_s (m^2 m^{-2}) is the area index of dead leaves, branches, stem and trunk which can be obtained by

$$L_s^n = \max\left\{\left[\beta \cdot L_s^{n-1} + \max\left(LAI_g^{n-1} - LAI_g^n, 0\right)\right], L_{s,\min}\right\} \tag{9}$$

where n denotes the nth LAI products with a 8-days temporal resolution; $L_{s,\min}$ (m^2 m^{-2}) is the prescribed minimum value of L_s; $(1-\beta)$ is the removal rate of dead leaves between two products. Both β and $L_{s,\min}$ are taken from literature [17] and given in Table I. Zeng *et al.* [17] has used a constant value of $L_{s,\min}$ in their study, while here we took it as varying values $L \cdot \max(FVC)$ changing with FVC in a pixel, and L is the value of $L_{s,\min}$ when $FVC = 1$.

The FVC was derived from NDVI following Bastiaanssesn *et al.* [18].

D. Poisson Distribution Function

A pixel is divided into several subpixels, and the FVC of any subpixel is equal to the FVC of the pixel. The probability of $VAI_{\text{sub}} = x$ of a subpixel is then given by

$$P(VAI_{\text{sub}} = x) = e^{-VAI_{\text{mean}}} \cdot VAI_{\text{mean}}^x / x! \quad (x = 0.01, 1, 2, 3, 4, \ldots) \tag{10}$$

where VAI_{mean} is the VAI of the pixel, VAI_{sub} is the VAI of subpixel following Poisson distribution.

E. Classification of Rainfall

As Miralles *et al.* [19] noted, the rainfall rate varies according to the type of storms. It is necessary to classify the rainfall events to reduce the impact of extreme cases on $\overline{R}$. The rainfall rates of convective (high intensity) and synoptic (low intensity) precipitation can be distinguished using a threshold of $\overline{R_t}$ with 2 mm h^{-1} [19]. Rainfall events with mean rainfall rates larger than $\overline{R_t}$ are classified into convective precipitation, the others are classified into synoptic precipitation.

IV. RESULTS AND ANALYSIS

A. Comparison With Ground Measurements

For there are only measurements in two forest sites available, the method will be verified over forest. As most pixels are not fully covered by forest, to allow comparison with the ground measurements of rainfall interception, the pixel-based estimates (as mm per unit area of land) must be converted to mm per unit area of forest [19]. The fraction of forest (FF) in the pixels of Dayekou and Pailugou experimental sites derived from the Hyperion image using the maximum likelihood classification approach was 0.8 and 0.61, respectively. Dividing the modeled interception ratio by FF, the interception ratio per unit area of forest is obtained.

TABLE II
STATISTICAL RESULTS OF MODELLED AND MEASURED MONTHLY INTERCEPTION RATIO (IN %) PER UNIT AREA OF THE TWO FOREST SITES FROM JUNE TO SEPTEMBER OF 2008

Date/Month	Dayekou		Pailugou	
	Modelled	measured	modelled	measured
06/2008	24.3	23.2	37.5	44.5
07/2008	22.5	23.4	37.7	36.3
08/2008	22.4	19.9	37.9	41.3
09/2008	15.0	23.7	20.4	28.5
Mean	21.1	22.6	33.4	37.7
STDEV	4.1	1.8	8.6	7.0
RMSE	5.0		4.3	

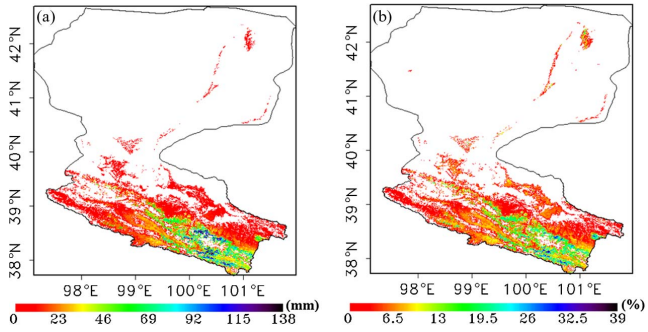

Fig. 2. Spatial patterns of (a) interception loss (mm/yr per unit area of land) and (b) interception ratio. Results are averaged over 2003–2012.

Table II shows the statistical results of the modeled and measured monthly interception ratio per unit area at the two forest sites, from June to September of 2008. The modeled interception ratio agrees well with the measurements with the RMSE of 5.0% at Dayekou experimental site and 4.3% at Pailugou experimental site. The modeled interception ratio is about 1.5% and 4.3% underestimated at the Dayekou and Pailugou experimental sites, respectively. However, the performance in other vegetation area cannot be verified directly due to the limitation of ground measurements in the study area. One point should be stated here is that the RS-Gash model is a modification of Gash analytical model for estimating regional interception loss, and the latter has been successfully used in different types of vegetation including rainforest, conifers, mixed conifer, shrubs and crops [16]. It is logic to assume that the RS-Gash model is also suitable for estimating the interception loss of shrub, grass and crop. In the next two sections, we would further discuss this issue.

B. Spatial Variability of Interception Loss

Fig. 2 presents the regional distribution of estimated interception loss of the main vegetation types in the Heihe River Basin during the 10 years period of 2003–2012. Absolute values of interception loss per year are shown in Fig. 2(a). Fig. 2(b) shows the interception ratio. The interception loss shows high spatial variability in particular in the upper reach of the basin, which can be attributed to the spatial heterogeneity of vegetation, meteorological factors and rainfall. The upper reach of the Heihe River Basin is dominated by forest and shrub with higher interception loss than other vegetation types (Fig. 3). The middle reach of the basin is dominated by crop and grass with lower interception loss comparing to the tall vegetation

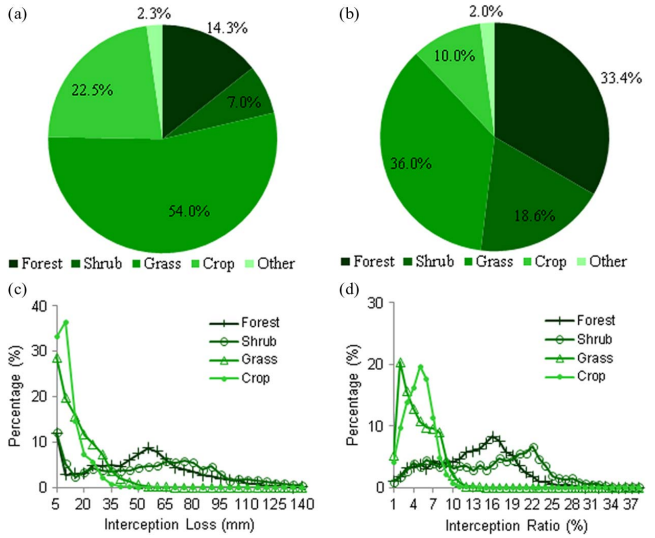

Fig. 3. Statistical results of (a) fraction of vegetation area, (b) fraction of interception loss of different vegetation, (c) histogram of the interception loss, and (d) histogram of the interception ratio. Results are averaged over 2003–2012.

(Fig. 3). The lower reach of the Heihe River Basin is dominated by desert with almost no interception loss due to scarce of rainfall (Fig. 2). For vegetation covered area in the Heihe River Basin, the annual average interception loss and gross rainfall are 19.8 mm/yr and 275.9 mm/yr, respectively, thus 7.2% of gross rainfall is intercepted by the vegetation.

Fig. 3(a) and (b) present statistical results of vegetation area and the interception loss of vegetation in percentage from 2003 to 2012. The magnitude order of the interception ratio per unit area of different vegetation types from high to low is: shrub (13.25%), forest (needle leaf and broad leaf) (12.74%), crop (4.08%), and grass (3.78%), as shown in the histograms of the interception loss [Fig. 3(c)] and of interception ratio [Fig. 3(d)]. Shrub has a little higher interception ratio than forest which is consistent with the observations of Liu *et al.* [20] who measured the interception ratio of four typical alpine shrubs (*Potentilla fruticosa*, *Salix cupularis*, *Hippophae rhamnoides*, and *Caragana jubata*) in the Qilian Mountains of the upper reach of Heihe River Basin in summer with a mean interception ratio of 35.8% (from 33.3% to 39.7%), much higher than the average value of the forest in Dayekou site (22.6%) and comparable with Pailugou (37.7%) site. This can be explained that the shrub has larger S_{Veg} than forest and the Heihe River Basin is dominated by light and small rainfalls.

The grass and crop have similar interception ratio, which are much lower than the forest and shrub due to the lower S_{Veg} and $\overline{E_V}$ for their aerodynamic resistances are much higher than tall vegetation [19]. However, it should be noted that the total interception loss of those two low vegetation types are still important as illustrated in our study since they occupy large area as dominant vegetation types in the Heihe River Basin.

C. Temporal Variability of Interception Loss

Fig. 4 presents the time series of interception loss and interception ratio of the main vegetation types per unit area of land in the Heihe River Basin. Fig. 4(a) and (c) show the annual average interception loss and interception ratio from

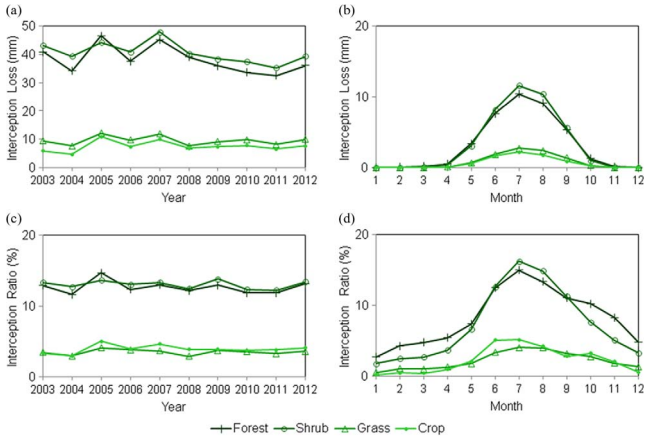

Fig. 4. Time series of interception loss and interception ratio of the main vegetation types per unit area of land in Heihe River Basin between 2003 and 2012. (a) The annual averaged interception loss (mm). (b) The monthly averaged interception loss of 10 years (mm). (c) The annual averaged interception ratio (%). (d) The monthly averaged interception ratio of 10 years (%).

2003 to 2012. We can see that interception ratio is more stable than the absolute value at annual scale. Fig. 4(b) and (d) show the monthly average interception loss and interception ratio from 2003 to 2012. All vegetation types show strong seasonal variability, indicating that both interception loss and interception ratio are higher in summer than that in winter. This can be explained by higher precipitation, VAI, FVC, and $\overline{E_V}$ in summer than that in winter. For the seasonal change of interception loss, the dominant factor is precipitation. As for interception ratio, VAI, FVC, and $\overline{E_V}$ are more critical.

V. Concluding Remarks

The validation at two forest sites showed that the RS-Gash model can estimate the interception loss with reasonable accuracy. For vegetation covered area in the Heihe River Basin, there is about 7.2% of gross rainfall lost due to vegetation interception. Although grass (3.48%) and crop (4.08%) have lower interception ratio than forest (12.74%) and shrub (13.25%), the interception loss of crop and grass are still important to water balance for the Heihe River Basin, for which occupy almost half of the total interception loss. At annual scale, the interception ratio is more stable than the absolute value of interception loss. At monthly scale, the interception has significant seasonal variability.

Some issues about using RS-Gash model to estimate the interception loss at regional scale need to be addressed here.

1) Since the localized S_V values for different vegetation types are not always available, we used the values of S_V from the previous studies which may be different from those in the study area.
2) The existence of mixing pixel is an unavoidable uncertainty sources for estimating the interception loss using remote sensing observations. An alternative method is to use high spatial resolution images to reduce the pixel-mixing effects.

Acknowledgment

The authors would like to thank to the useful comments from the guest editors X. Li, S. M. Liu, and R. Jin. The authors gratefully acknowledge the anonymous reviewers for their valuable comments that improve the quality of this letter.

References

[1] R. G. Allen, "Using the FAO-56 dual crop coefficient method over an irrigated region as part of an evapotranspiration intercomparison study," *J. Hydrol.*, vol. 229, no. 1/2, pp. 27–41, Mar. 2000.
[2] H. H. Bulcock and G. P. W. Jewit, "Modelling canopy and litter interception in commercial forest plantations in South Africa using the variable storage gash model and idealized dry curves," *Hydrol. Earth Syst. Sci.*, vol. 16, no. 12, pp. 4693–4705, Dec. 2012.
[3] A. I. J. K. vanDijk and L. A. Bruijnzeel, "Modelling rainfall interception by vegetation of variable density using an adapted analytical model. Part 2. Model validation for a tropical upland mixed cropping system," *J. Hydrol.*, vol. 247, no. 3/4, pp. 239–262, Jul. 2001.
[4] D. Levia and E. Frost, "Variability of throughfall volume and solute inputs in wooded ecosystems," *Prog. Phys. Geogr.*, vol. 30, no. 5, pp. 605–632, Oct. 2003.
[5] M. Motahari, P. Attarod, and T. G. Pypker, "Rainfall interception in a Pinus eldarica plantation in a semiarid climate zone: An application of the gash model," *J. Agr. Sci. Technol.*, vol. 15, no. 5, pp. 981–994, Sep. 2013.
[6] W. J. Shuttleworth and J. S. Wallace, "Evaporation from sparse crops—An energy combination theory," *Q. J. R. Meteorol. Soc.*, vol. 111, no. 469, pp. 839–855, Jul. 1985.
[7] A. M. J. Gerrits, L. Pfsiter, and H. H. G. Savenije, "Spatial and temporal variability of canopy and forest floor interception in a beech forest," *Hydrol. Process.*, vol. 24, no. 21, pp. 3011–3025, Oct. 2010.
[8] J. H. C. Gash, "Estimating sparse forest rainfall interception with an analytical model," *J. Hydrol.*, vol. 170, no. 1–4, pp. 79–86, Aug. 1995.
[9] H. Mathias, T. W. R. Paul, and D. M. David, "Seasonal variability of interception evaporation from the canopy of a mixed deciduous forest," *Agr. Forest Meteorol.*, vol. 148, no. 11, pp. 1655–1667, Oct. 2008.
[10] X. Li *et al.*, "Watershed allied telemetry experimental research," *J. Geophys. Res.*, vol. 114, no. D22, pp. D22103-1–D22103-19, Nov. 2009.
[11] X. Li *et al.*, "Heihe Watershed Allied Telemetry Experimental Research (HiWATER): Scientific objectives and experimental design," *Bull. Amer. Meteorol. Soc.*, vol. 94, no. 8, pp. 1145–1160, Aug. 2013.
[12] Y. K. Cui and L. Jia, "A modified gash model for estimating rainfall interception loss of forest using remote sensing observations at regional scale," *Water*, vol. 6, no. 4, pp. 993–1012, Apr. 2014.
[13] X. D. Pan *et al.*, "Dynamic downscaling of near-surface air temperature at the basin scale using WRF—A case study in the Heihe River Basin, China," *Frontiers Earth Sci.*, vol. 6, no. 3, pp. 314–323, Sep. 2012.
[14] L. Jia, H. L. Shang, G. C. Hu, and M. Menenti, "Phenological response of vegetation to upstream river flow in the Heihe River basin by time series analysis of Modis data," *Hydrol. Earth. Syst. Sci.*, vol. 15, no. 3, pp. 1047–1064, Jul. 2011.
[15] Y. H. Ran, X. Li, L. Lu, and Z. Y. Li, "Large-scale land cover mapping with the integration of multi-source information based on the Dempster-Shafer theory," *Int. J. Geogr. Inf. Sci.*, vol. 26, no. 1, pp. 169–191, Jan. 2012.
[16] A. Muzylo, P. Llorens, and F. Valente, "A review of rainfall interception modeling," *J. Hydrol.*, vol. 370, no. 1–4, pp. 191–206, May 2009.
[17] X. Zeng, M. Shaikh, and Y. Dai, "Coupling of the common land model to the NCAR community climate model," *J. Clim.*, vol. 15, no. 14, pp. 1832–1854, Jul. 2002.
[18] W. G. M. Bastiaanssen, M. J. M. Cheema, W. W. Immerzeel, I. J. Miltenburg, and H. Pelgrum, "Surface energy balance and actual evapotranspiration of the transboundary Indus Basin estimated from satellite measurements and the ETLook model," *Water Resourc. Res.*, vol. 48, no. 11, pp. W11512-1–W11512-16, Nov. 2012.
[19] D. G. Miralles, J. H. Gash, and T. R. H. Holmes, "Global canopy interception from satellite observations," *J. Geophys. Res.*, vol. 115, no. D16, pp. D16122-1–D16122-8, Aug. 2010.
[20] Z. W. Liu, R. S. Chen, Y. X. Song, and C. T. Han, "Characteristics of rainfall interception for four typical shrubs in Qilian Mountain," *Acta Ecol. Sin.*, vol. 32, no. 4, pp. 1337–1346, Feb. 2012.